AIMS Environmental Science, 10(3): 325–340.
DOI: 10.3934/environsci.2023019
Received: 26 December 2022
Revised: 02 April 2023
Accepted: 04 April 2023
Published: 17 April 2023

http://www.aimspress.com/journal/environmental

Research article

Experimental evaluation of lime spray drying for SO_2 absorption

Lawrence Koech[1,2,*], Hilary Rutto[1,2] and Tumisang Seodigeng[1]

[1] Department of Chemical and Metallurgical Engineering, Vaal University of Technology, Vanderbijlpark Campus, Private Bag X021, 1911, South Africa

[2] Eskom Power Plant Engineering Institute (EPPEI) Specialization Centre for Emission Control, School of Chemical and Minerals Engineering, Centre of Excellence in Carbon-based Fuels, North-West University, Private Bag X6001, Potchefstroom 2520, South Africa

* **Correspondence:** Email: lawrencek@vut.ac.za; Tel: 016 950 6742.

Abstract: This paper presents the findings of an experimental investigation on the performance of a laboratory-scale spray dryer involving flue gas desulfurization. Using commercial hydrated lime as a sorbent, a systematic set of experiments were performed to evaluate SO_2 absorption capacity of the spray dryer. The experimentation involved accurate measurement of the spray drying characteristics, such as temperature and SO_2 concentration along the spray chamber, by varying the input and output variables. Tests were done to investigate the effects of spray characteristics, i.e., inlet gas phase temperature (120–180 ℃) and calcium-to-sulfur ratio (1–2.5), on SO_2 removal efficiency. The performance of the spray dryer was further evaluated based on the degree of conversion of calcium (sorbent utilization) after SO_2 absorption. Results indicated an increase in SO_2 removal efficiency by increasing the stoichiometric ratio and decreasing the temperature. Absorption efficiency of SO_2 beyond 90% was achieved at a stoichiometric ratio of 2.5. A high degree of conversion of calcium was realized at low stoichiometric ratios, with a maximum utilization of 94% obtained at a stoichiometric ratio of 1.5. The analysis of the final desulfurization product revealed the presence of sulfite with better conversion achieved at a stoichiometric molar ratio of 1.5. A significant amount of unreacted sorbent (63.43%) was observed at a stoichiometric ratio of 2, while samples collected at a stoichiometric ratio of 1.5 had the lowest concentration of unreacted $Ca[OH]_2$ (41.23%).

Keywords: spray drying absorption; hydrated lime; desulfurization; SO2 in air; sorbent conversion

Abbreviations: BET: Branauer-Emmett-Teller; BJH: Barrett-Joyner-Halenda; EDS: Energy dispersive spectroscopy; FGD: Flue gas desulphurization; FTIR: Fourier transform infrared; IUPAC: International Union of Pure and Applied Chemistry; SDA: Spray drying absorption; SEM: Scanning electron microscopy; SR: Stoichiometric ratio; TGA: Thermogravimetric analyzer; TG/DTA: Thermogravimetry Differential Thermal Analysis; XRD: X-ray diffraction; XRF: X-ray fluorescence

1. Introduction

Flue gas desulfurization (FGD) is a scrubbing system that has been predominantly used worldwide for mitigation of SO_2 emissions from flue gases in industries. It utilizes a sorbent material to interact with flue gas containing sulfur dioxide (SO_2) within the absorber or scrubber to generate a dense sulfur slurry [1]. Typically, an alkali-rich sorbent containing either Mg or Ca reacts with SO_2, forming a solid end product with ease of disposal. This makes lime ($Ca[OH]_2$) and limestone ($CaCO_3$) the most widely used sorbents in FGD processes due to their availability and calcium abundance. Among others, magnesium, seawater, sodium and amine are used as sorbents for FGD.

The spray drying absorption (SDA) process is classified as a semi-dry FGD system comprising slurry preparation, the scrubbing chamber, particulate collection and management of the end product. This scrubbing technique employs either limestone ($CaCO_3$), hydrated lime ($Ca[OH]_2$) or sodium carbonate (Na_2CO_3) slurries prepared by continuously mixing with water to avoid sedimentation and agglomeration [2]. Hydrated lime slurry is widely utilized in this process, chiefly because it is more reactive toward SO_2 than limestone and it is less expensive than Na_2CO_3. The prepared slurry enters through the top of the scrubber via the spray nozzles or atomizers where it is dispersed, forming fine droplet mists carrying $Ca[OH]_2$. The dispersal of the slurry provides greater interaction of the hot flue gas and the lime slurry droplets within the spray chamber. As the flue gas descends through the chamber, $Ca[OH]_2$ in the slurry droplets reacts with the SO_2 in the flue gas to form a dry solid product predominantly consisting of $CaSO_3$ and traces of $CaSO_4$ [3,4].

The spray drying absorption process for FGD is an inexpensive retrofit SO_2 control technology best suited for pre-existing coal-fired power plants. It is increasingly becoming an attractive alternative due to the ease of handling the dry end product and smaller footprint requirement as compared to wet FGD systems [5–7]. However, it has low sorbent conversion and low SO_2 removal capabilities in comparison to the well-established wet limestone FGD process. The removal efficiency of SO_2 in this process rarely surpasses 70% when a calcium-to-sulfur ratio of 1:2 is used, and this has restricted its application to power plants using coal with low sulfur content [7]. The SDA process requires the use of a high stoichiometric ratio (i.e., Ca:S ratio) to attain the required SO_2 removal limits, consequently resulting in low sorbent utilization. Lower SO_2 removal efficiency in SDA is also ascribed to the brief period when the droplet is still wet (constant rate drying period). In this period, there is substantial removal of SO_2 preceding the falling rate drying period in the chamber where minimal or no SO_2 removal occurs [8].

The study consisted of sets of experiments conducted to integrate drying, evaporation and SO_2 absorption by varying the inlet gas temperature (120–180 °C), slurry solid content (6–12%) and calcium-to-sulfur molar ratio (1–2.5). A critical part of this study involved accurate measurement of the process conditions within the spray dryer to obtain both axial profiles while controlling the input and output variables, such as flow rates, inlet temperatures, sorbent utilization and efficiency (calculated). The analysis of the final desulfurization product is also crucial in determining the utilization of the sorbent in a spray drying FGD system.

2. SO_2 reactions in lime spray dryer

During the reaction process, the interaction between $Ca[OH]_2$ in the droplet and SO_2 from the gas bulk takes place simultaneously, resulting in a string of reactions and eventually drying of the reacted products. The absorption of SO_2 into $Ca[OH]_2$ slurry is an instantaneous reaction involving multiphase absorption processes, which include the diffusion of solute gas, the dissolution of $Ca[OH]_2$ particles and chemical reactions [9]. The absorption of SO_2 in a lime spray dryer follows the reaction path described below [7,10,11]:

a) SO_2 diffusion, absorption and subsequent formation of sulfurous acid:

$$SO_{2(g)} \leftrightarrow SO_{2(aq)} \tag{1}$$

$$SO_{2(g)} + H_2O_{(l)} \rightarrow H_2SO_{3(aq)} \tag{2}$$

b) Dissociation into ionic sulfur species:

$$H_2SO_{3(aq)} \leftrightarrow H^+_{(aq)} + HSO^-_{3(aq)} \tag{3}$$

$$HSO^-_{3(aq)} \leftrightarrow H^+_{(aq)} + SO^{2-}_{3(aq)} \tag{4}$$

c) Dissolution of $Ca[OH]_2$ particles into alkaline species:

$$Ca(OH)_{2(s)} \rightarrow Ca^{2+}_{(aq)} + OH^-_{(aq)} \tag{5}$$

d) Neutralization reaction between alkaline and acid species:

$$H_2SO_{3(aq)} + 2OH^-_{(aq)} \rightarrow SO^{2-}_{3(aq)} + 2H_2O_{(l)} \tag{6}$$

$$HSO^-_{3(aq)} + 2OH^-_{(aq)} \rightarrow SO^{2-}_{3(aq)} + H_2O_{(l)} \tag{7}$$

e) Reaction to form calcium sulfate hemihydrate:

$$Ca^{2+}_{(aq)} + SO^{2-}_{3(aq)} + H_2O_{(l)} \rightarrow 2CaSO_3.\frac{1}{2}H_2O_{(s)} \tag{8}$$

3. Materials and methods

A systematic experimentation program was used to evaluate the SO_2 absorption behavior of the spray dryer by varying the main operating variables in addition to controlling the input and output variables, such as flow rates, temperature concentrations and efficiency. The range of process conditions used for this study is presented in Table 1. All experiments in this study were performed using a laboratory-scale Buchi B290 Mini Spray Dryer. A schematic of the experimental setup is shown in Figure 1, and it comprises the following main systems.

3.1. Slurry preparation

Lime slurry was prepared using commercial hydrated lime by mixing it externally with an appropriate proportion of water in a vessel. The contents in the vessel were stirred constantly to inhibit sedimentation and agglomeration. The contents of the vessel were then supplied continuously into the

spray chamber via the spray nozzle in the spray chamber. Compressed air was used to atomize (disperse) the slurry into fine droplets which are subsequently dried in the spray chamber. The chemical composition of the hydrated lime used is presented in Table 2.

3.2. Spray drying chamber

The spray dryer consisted of a unit that regulates the air flow rate, inlet gas temperature and the slurry flow rate into the reaction chamber. The spray chamber was 0.6 m high and 0.16 m in diameter and made of borosilicate glass 3.3, providing a gas mean residence time of 1.0–1.5 seconds. The spray dryer was also equipped with an electric heater to provide the desired temperature in the inlet gas. SO_2 gas was dosed into the inlet air stream at a controlled rate to simulate the typical conditions prevailing in industrial flue gas streams. The temperature of the flue gas was monitored at the points of entry and exit to the chamber. The flow rates of both SO_2 and the ambient air streams were regulated using appropriate flow meters to achieve the desired SO_2 concentration in the simulated flue gas.

The slurry was introduced into the spray chamber through a two-fluid nozzle which disperses the slurry, producing droplets which then interact with hot flue gas in co-current flow. The stoichiometric ratio was controlled by varying the slurry solid concentration. The flue gas temperature, relative humidity and SO_2 concentration were measured at various positions along the spray chamber height to obtain their respective profiles as shown in Figure 1.

3.3. Flue gas analysis

The simulated flue gas was prepared by mixing 99% SO_2 with inlet air by means of flow controllers to maintain the desired flue gas volume flow and inlet concentration of SO_2. The concentration of SO_2 in the gas stream was analyzed using a Testo 340 combustion gas analyzer. The desulfurization efficiency was determined directly on the basis of concentrations of SO_2 at the inlet and outlet.

$$\eta = \frac{N_{SO_{2,i}} - N_{SO_{2,o}}}{N_{SO_{2,i}}} \tag{9}$$

Where $N_{SO_{2,i}}$ and $N_{SO_{2,o}}$ are the mole flows of SO_2 entering and leaving the spray chamber, respectively.

To ensure data accuracy, experiments were conducted in triplicate and data collection commenced only when a steady state was achieved. Standard deviation was then calculated for all data collected.

3.4. Characterization

The Branauer-Emmett-Teller (BET) surface area and Barrett-Joyner-Halenda (BJH) pore volume of the hydrated lime sorbent were determined from the N_2 adsorption-desorption isotherms at 77 K using a Micromeritics ASAP™ 2020 Porosity Analyzer. Qualitative analysis of the sorbent was determined by an x-ray diffraction (XRD) technique using a Malvern Panalytical Aeris diffractometer with a PIXcel detector and fixed slits with Fe-filtered Co-Kα radiation. The phases present were identified using X'Pert Highscore plus software. The functional groups present in the final desulfurization product were determined by Fourier transform infrared (FTIR) analysis using a Perkin-Elmer Spectrum Two™ machine. A scanning electron microscopy (SEM) machine equipped with energy dispersive spectroscopy (EDS) was used to determine the morphological structures of the samples, and to detect the chemical elemental composition on the surface of the final desulfurization

product. The decomposition properties of various compounds in the final desulfurization products were assessed using an SDT Q600 TGA analyzer.

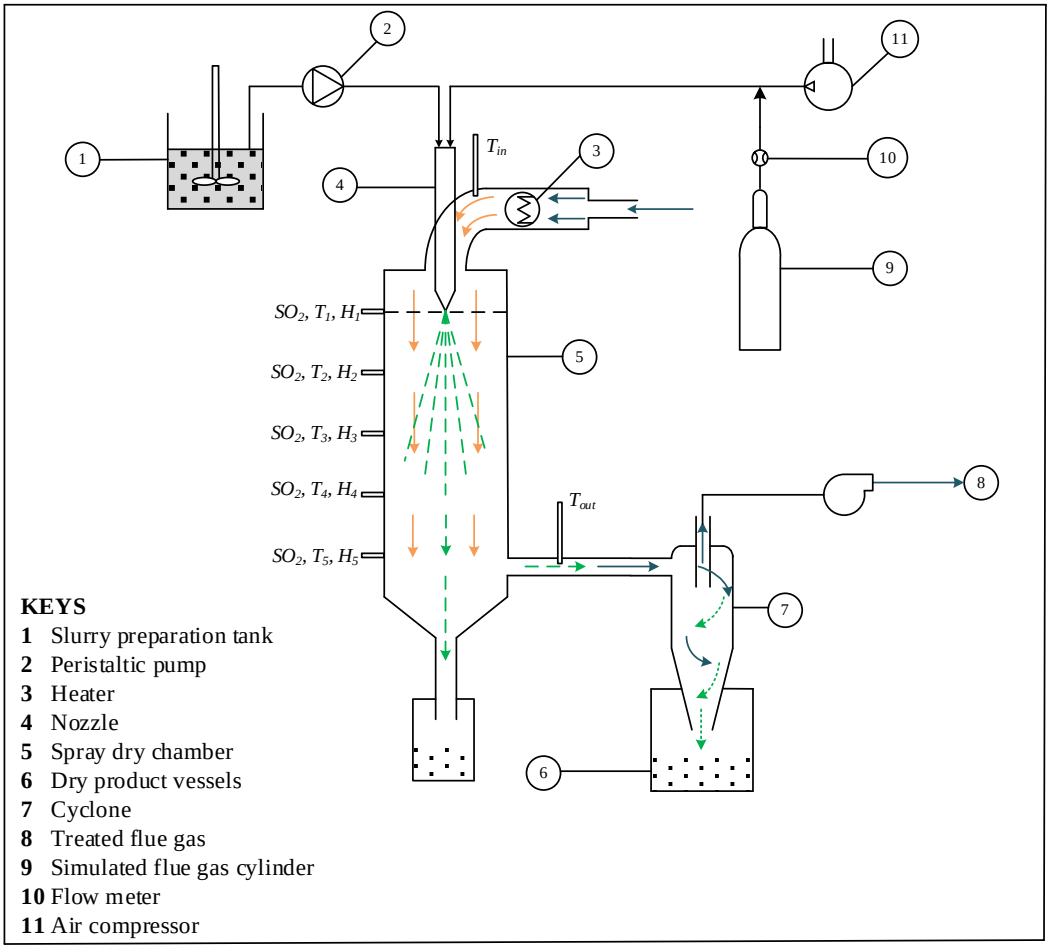

Figure 1. Lime spray drying experimental setup.

Table 1. Experimental conditions.

Variables	Ranges
Inlet air temperature (°C)	120–180
Feed air flow rate (m^3/h)	20–35
Slurry solid concentration (%)	6–12
Atomizing air flow rate (l/h)	350–750
Calcium-to-sulfur (stoichiometric) ratio	1–2.5
Flue gas SO_2 concentration (ppm)	500–2000

4. Results and discussion

4.1. Sorbent's physical and chemical properties

The chemical composition of hydrated lime determined by x-ray fluorescence (XRF)analysis is given in Table 2. From the analysis, the sorbent is mainly composed of CaO with a content of 89.55%, which is crucial in the total sulfation of the sorbent. Impurities consisted of SiO_2, MgO and Al_2O_3, with trace amounts of K_2O, Mn_3O_4, TiO_2 and Na_2O.

Table 2. Chemical composition of hydrated lime.

	Content wt.%								
	SiO_2	Al_2O_3	K_2O	Mn_3O_4	CaO	MgO	TiO_2	Na_2O	SrO
Lime	7.38	0.79	0.05	0.12	89.55	1.12	0.06	0.23	0.19

The XRD pattern in Figure 2 revealed portlandite ($Ca[OH]_2$) as a major crystalline phase in the sorbent. The analysis also indicated the presence of quartz crystalline phase, which appears as a mild hump on the diffraction patterns. The specific surface area determined by BET surface area analysis was found to be $4.24\,m^2/g$. The adsorption/desorption isotherm plot in Figure 3 indicates that the sorbent used belongs to a typical type II isotherm, in accordance with International Union of Pure and Applied Chemistry (IUPAC) classification. This indicates a multilayer adsorption property associated with microporous materials [12]. This demonstrates that the sorbent particles can be classified as mesopores bearing pore diameters greater than micropores. Particles with pore sizes ranging from 2–100 μm are recognized to be effective in the sulfation reaction between sulfur and alkaline species [13,14].

4.2. Spray drying desulfurization variables

4.2.1. Effect of stoichiometric ratio on SO_2 absorption

The stoichiometric ratio (SR) is an expression for the ratio of moles of fresh sorbent to the moles of SO_2 in the flue gas. It is an indication of the rate of consumption of the sorbent, which is a critical economic consideration in the process. It is also one of the key parameters necessary during the design stage of a spray dryer [2]. For the lime spray drying process, the stoichiometric ratio is evaluated as

$$SR = \frac{Moles\ of\ Ca(OH)_2\ in\ feedslurry}{Moles\ of\ SO_2\ in\ flue\ gas} \tag{10}$$

In this study, experiments were conducted by varying the stoichiometric ratio from 1 to 2.5 at a constant temperature of 140 °C. This was varied by regulating the amount of $Ca[OH]_2$ in the feed slurry. The results of this experiment are represented in Figure 4. The results indicate a rapid rise in the desulfurization efficiency with an increase in the stoichiometric ratio, and this is attributed to the increase in the slurry concentration, which reduces the droplet liquid-phase mass transfer resistance for SO_2 [7,15]. A high SO_2 absorption efficiency beyond 80% was achieved for a stoichiometric ratio of 2.5. However, the economic analysis of lime and solid waste disposal costs requires lower stoichiometric ratios for this process [16]. Furthermore, high stoichiometric ratios lead to poor sorbent utilization, owing to the typical property of the lime slurry droplets in the reaction chamber where the reaction products cover the outer parts while the core of the droplet remains unreacted.

The results also indicate an almost linear increase in SO_2 absorption from the nozzle tip before it levels off toward the exit of the spray chamber for the range of the stoichiometric ratio used. As the droplet leaves the nozzle, there is a high concentration of lime particles near the droplet surface, which reduces the liquid-phase mass transfer resistance [15]. As the droplet continues to drop, additional external resistances due to mass transfer or liquid-phase mass transfer of the reactant species (sulfur) through the product layer of $CaSO_3$ will limit the absorption of SO_2. This is evident in the levelling of the graphs toward the exit of the spray chamber for a stoichiometric ratio between 1.5 and 2.5.

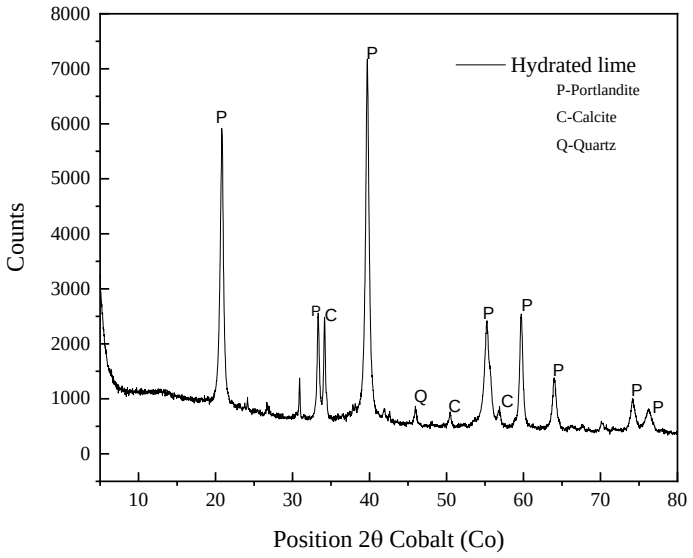

Figure 2. XRD diffraction pattern for hydrated lime.

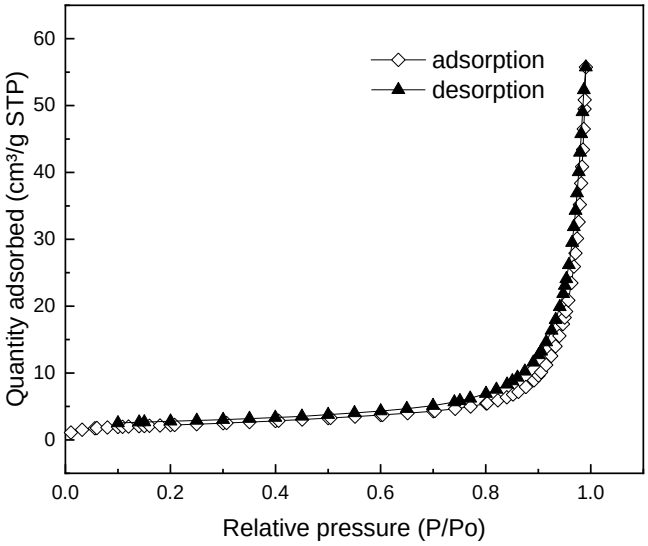

Figure 3. Nitrogen adsorption/desorption isotherm linear plot for hydrated lime.

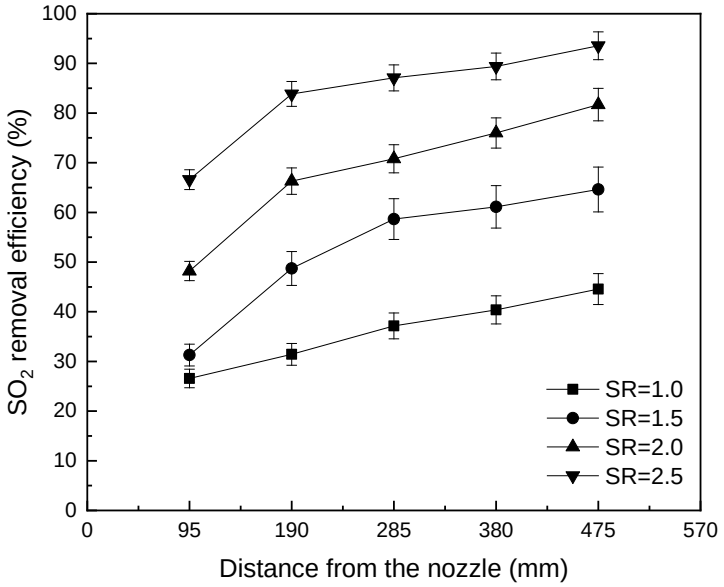

Figure 4. The effect of the stoichiometric ratio on SO_2 removal efficiency (inlet air flow rate, 35 m^3/h; slurry federate, 15 ml/min; temperature, 140 °C).

4.2.2. Effect of inlet gas phase temperature on SO_2 absorption

The absorption of SO_2 was studied with varying inlet gas temperatures ranging from 120 to 180 °C at a constant stoichiometric ratio of 1.5. These temperatures corresponded to outlet temperature values of 35 and 48 °C, respectively. Figure 5 shows the experimental findings, where it was observed that an increase in the inlet gas temperature causes a decrease in the absorption efficiency of SO_2. This is attributed to the accelerated drying rate caused by an increased gas-phase temperature in the spray chamber. Higher inlet gas temperatures create a substantial temperature difference between the bulk gas and the droplets, which causes rapid evaporation and subsequently reduces the necessary contact time for the chemisorption reaction [2,7]. The highest SO_2 removal efficiencies beyond 80% were obtained for temperatures of 120 and 140 °C at the chamber height of $z = 485mm$. This is because lower temperatures allowing a close temperature difference between the gas bulk and the droplet is necessary to provide an adequate lifetime for SO_2 absorption because of reduced evaporation.

In the spray chamber, the reactivity of the slurry droplet toward SO_2 is strongly dependent on the moisture retention capacity of the droplet. The reactions, as shown in Eqs 1–8, are considered to occur in the aqueous phase, and thus rapid moisture loss through evaporation hinders the necessary reactions [10]. These reactions are instantaneous in the presence of water but extremely slow in the absence of water. This is evident in the SO_2 absorption findings, as shown in Figure 5, where there is a steady rise in the absorption efficiency at the top section of the spray dryer ($285mm$) before almost levelling off toward the chamber exit. The steady rise in the absorption of SO_2 over the range of temperatures is attributed to a constant rate drying period where the droplet still contains sufficient moisture for chemisorption reaction [17]. As the droplet leaves the atomizer, rapid evaporation begins and consequently concentrates lime particles inside the droplet. SO_2 diffuses from the gas-phase region to the moist film on the droplet surface containing $Ca[OH]_2$ particles and reacts with the dissolved alkaline species. A reaction product will then be formed, precipitating on the droplet surface, which forms a barrier restricting both moisture vaporization and the absorption of SO_2 [18].

In this study, a dry simulated flue gas was used to simplify the experimental conditions and isolate the effect of inlet gas temperature on SO_2 removal efficiency. However, in real industry processes, the moisture content in flue gas can vary depending on the type of fuel and the combustion conditions.

Typically, the moisture content can range from 12% to 16% in volume [19]. The presence of moisture content can affect the heat and mass transfer in the reaction chamber, behavior of lime particles and the SO_2 absorption process, leading to changes in the overall efficiency of the system [20].

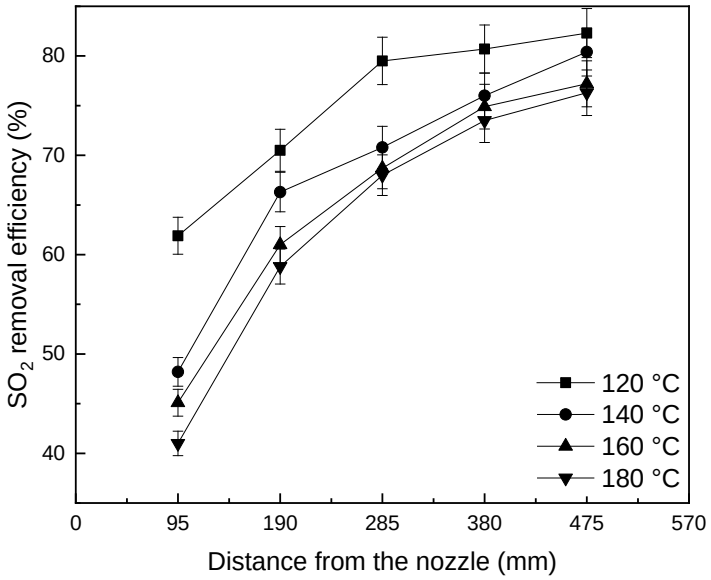

Figure 5. SO_2 removal efficiency at different temperatures (inlet air flow rate, 35 m^3/h; lime slurry solid concentration, 6%; slurry feed rate, 15 ml/min).

4.2.3. Sorbent utilization

The performance of the spray dryer was also evaluated based on the degree of conversion of calcium (calcium utilization) after SO_2 absorption, which is calculated as [21]

$$x_{Ca} = \frac{N_{SO_{2,i}} - N_{SO_{2,o}}}{N_{Ca_i}} \tag{11}$$

Where,

$N_{SO_{2,i}}$ is the mole flow of SO_2 in the entering gas.

$N_{SO_{2,o}}$ is the mole flow of SO_2 in the exiting gas.

N_{Ca_i} is the mole flow of calcium in the feed slurry.

Figure 6 represents the experimental results for the influence of inlet gas phase temperature (140–180 °C) and stoichiometric ratio (1.0–2.5) on the degree of conversion of calcium and SO_2 removal efficiency. The results show a decreasing degree of conversion of calcium and SO_2 removal efficiency with increasing temperature. Higher temperatures accelerate the droplet evaporation rate, thereby limiting its lifetime for both calcium conversion and SO_2 absorption. Experimental results also show that a high degree of conversion of calcium was achieved at low stoichiometric ratios. The maximum value of 94% was obtained at a stoichiometric ratio of 1.5 for an inlet gas temperature of 140 °C. The results also indicate increasing SO_2 absorption efficiency with increasing stoichiometric ratio due to negligible internal mass transfer resistances for SO_2 at high stoichiometric ratios [11]. It is, however, advisable to operate the spray dryer with a minimum stoichiometric ratio to reduce the operating cost and wet deposition on the walls of the chamber [22].

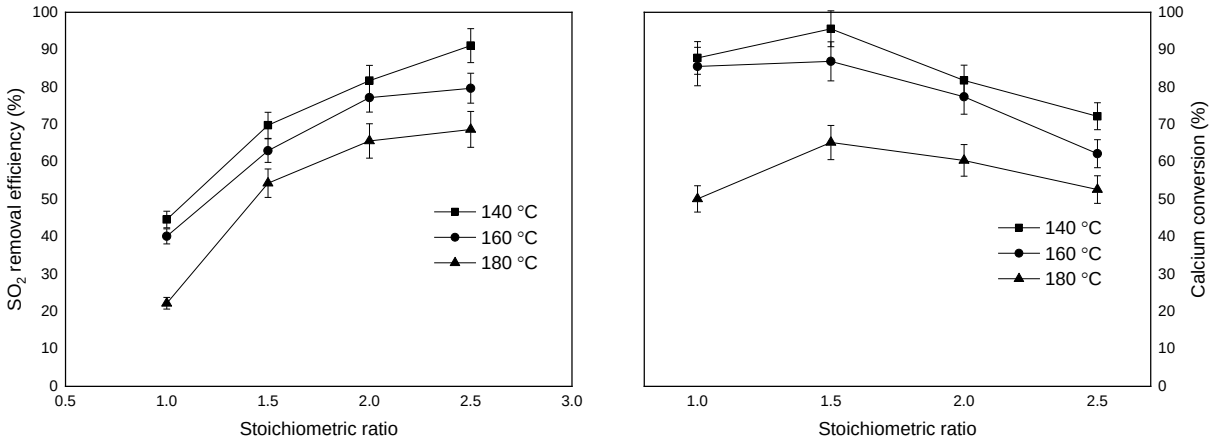

Figure 6. The effect of the Ca:S ratio and inlet gas temperatures on SO_2 removal efficiency (%) and calcium conversion (%), respectively.

4.3. Characterization of the spray drying product

4.3.1. SEM and EDS analysis

The surface morphologies of the final dried products after desulfurization obtained by SEM analysis were used to assess the influence of the spray drying conditions on the hydrated lime particles. Figure 7 shows the micrographs obtained under varying stoichiometric molar ratios of 1.0, 1.5 and 2.0, respectively. It was observed from the micrographs that the samples obtained at a stoichiometric ratio of 1.0 and 2.0 had porous irregular particles with relatively rough surfaces. This property is attributed to products of the desulfurization and agglomeration of partially reacted sorbent particles forming larger aggregates [21]. Extensive agglomeration was observed on the sample obtained at a stoichiometric ratio of 2.0, which retained higher moisture content on the surface of the sorbent, leading to higher desulfurization activity. The sample obtained at a stoichiometric ratio of 1.5 was observed to be plate-like and needle-like shaped particles, which are typical of calcium sulfite and gypsum particles [23]. They are also mainly composed of depleted sorbent particles after a reaction with SO_2. This observation corresponds with the experimental findings where the highest sorbent utilization of 94% was realized at a stoichiometric ratio of 1.5.

Table 3. Surface chemical composition by EDS analysis.

	$SR = 1.0$	$SR = 1.5$	$SR = 2.0$
Ca	64.19	65.87	68.50
S	4.72	8.95	7.79
O	31.09	25.18	23.71
Total	100.00	100.00	100.00

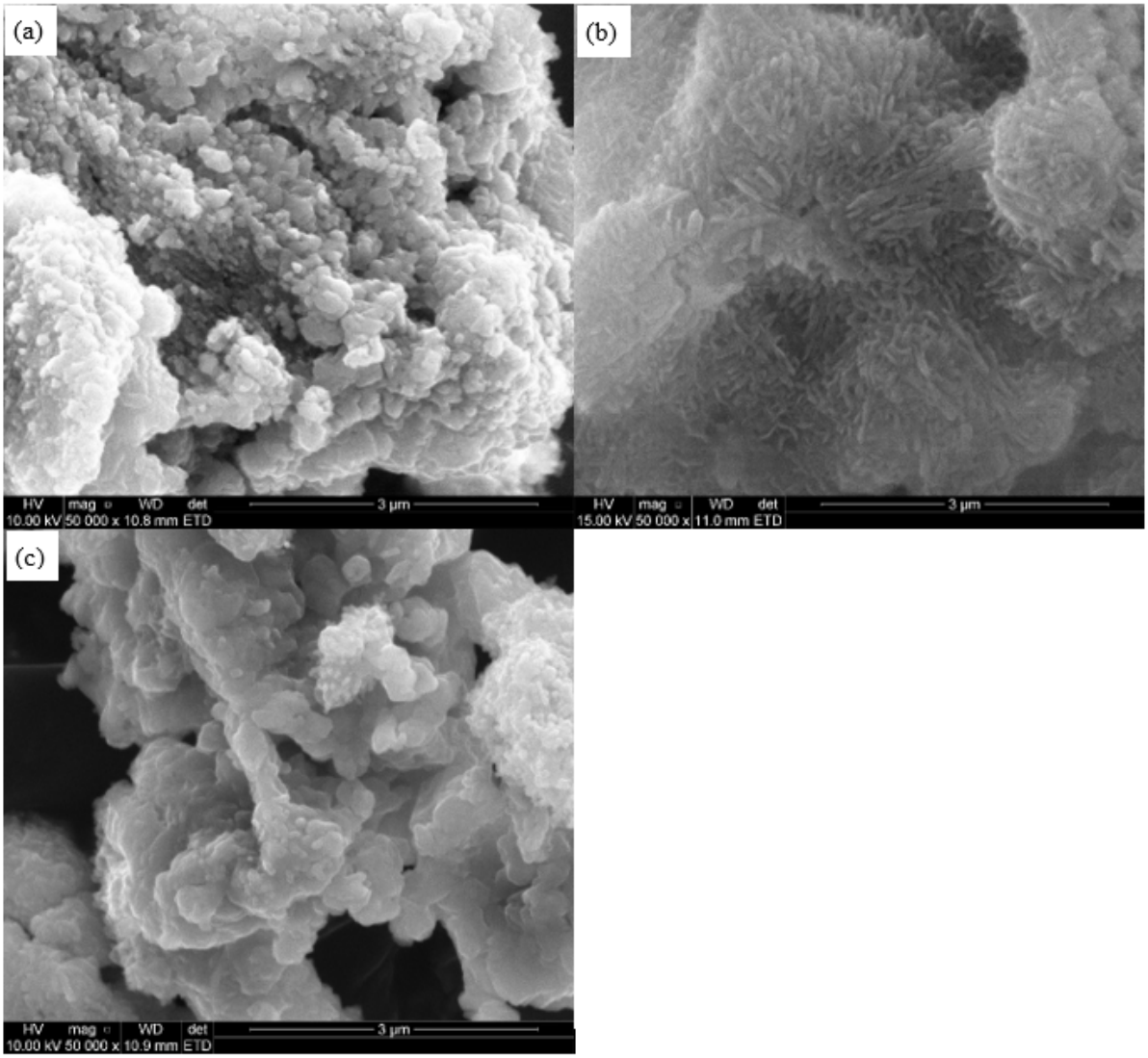

Figure 7. SEM micrographs for desulfurization products obtained at (a) $SR = 1.0, (b) SR = 1.5$, and (c) $SR = 2.0$.

The samples were further tested by EDS analysis to obtain their respective normalized elemental compositions as presented in Table 3. The elemental compositions indicated an increased concentration of calcium mass percentage (from 64.19 to 68.5%) with an increasing stoichiometric molar ratio. This is mainly due to the increased concentration of lime introduced into the feed slurry to achieve the required stoichiometric ratio. The results also indicate the highest concentration of sulfur (8.95% by mass) for the sample collected at a stoichiometric ratio of 1.5 compared to the samples collected at a stoichiometric ratio of 1.0 and 2.0, which contained 4.72 and 7.79 mass percentages, respectively. The presence of the sulfur element in the dried product indicates the absorption of SO_2 into the sorbent to form SO_3 and SO_4 salts (i.e., $CaSO_3$ and $CaSO_4$). A high concentration of sulfur on the final product at a stoichiometric ratio of 1.5 is due to high desulfurization activity per mass of the sorbent. This led to improved sorbent conversion, which was confirmed by the theoretical evaluation of the degree of conversion at different stoichiometric ratios. Based on EDS analysis and the evaluation of sorbent utilization, it can therefore be concluded that effective utilization of the of hydrated lime in the spray dryer can be achieved when a stoichiometric ratio of 1.5 is used.

4.3.2. FTIR analysis

Samples of the dried product collected after desulfurization were analyzed using FTIR with a spectral range of 4500–350 cm^{-1}. Figure 8 illustrates the FTIR analysis spectra of the desulfurization products at different stoichiometric ratios ranging from 1.0 to 2.0. The spectral profiles, as seen in the figure, show a strong broad absorption band around 938 cm^{-1} and at 650 cm^{-1}, which are assigned to calcium sulfite hemihydrate [24]. The sulfate ions had a characteristic minor absorption band at 1120–1170 cm^{-1} [25]. As observed in the spectra, the sample collected at a stoichiometric ratio of 1.5 had a huge calcium sulfite hemihydrate spectrum at 938 cm^{-1}. This is due to the significant proportion of sulfite formed in the final product resulting from high sorbent conversion, as observed at a stoichiometric ratio of 1.5. This was confirmed by the chemical analysis, which revealed a strong presence of 24.57% $CaSO_3 \cdot 0.5H_2O$ in the final desulfurization product. The infrared profiles also show significant changes in the absorption bands around 1413 and 3642 cm^{-1}, which were identified as calcite and portlandite, respectively [26]. The conversion of the sorbent accounts for the changes in the infrared absorption bands for portlandite and calcite at different stoichiometric ratios, as illustrated in Figure 8. The depleted portlandite peak for the collected sample at a stoichiometric ratio of 1.5 is evidence of high sorbent conversion, with corresponding huge peaks at around 938 cm^{-1} for sulfite. The highest portlandite peaks at stoichiometric ratios of 1.0 and 2.0 demonstrate significant proportion of unreacted sorbent, as confirmed by EDS analysis and the evaluation of unreacted $Ca[OH]_2$ by TGA analysis.

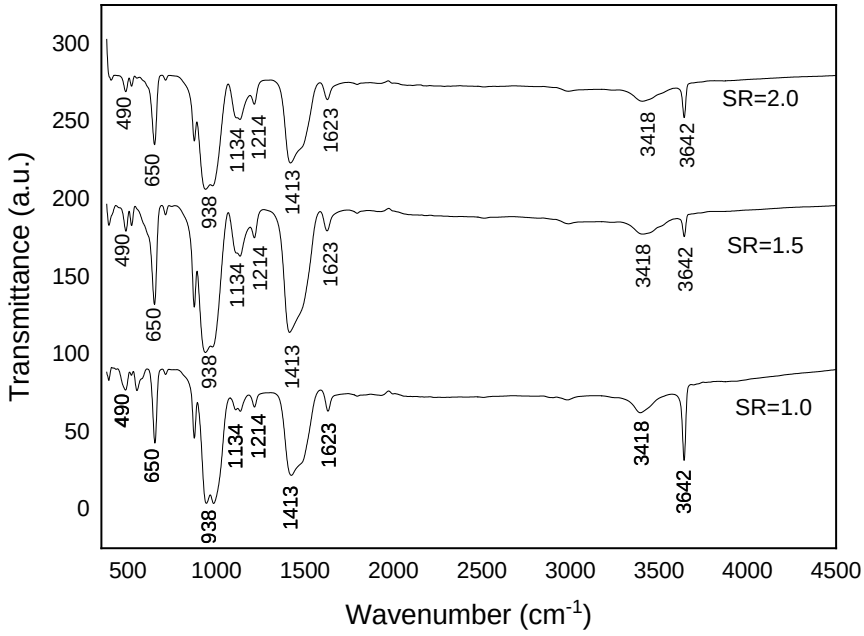

Figure 8. FTIR spectra for desulfurization products under varying stoichiometric ratios.

4.3.3. Evaluation of unreacted $Ca[OH]_2$ by TGA analysis

Thermogravimetric analysis of the final product was conducted to verify and assess the decomposition of various compounds at different temperatures. Different samples of the final desulfurization product were collected under varying experimental conditions (i.e., with SR of 1.0, 1.5, and 2.0) and analyzed by TGA. Their composition was evaluated based on the weight loss at different temperatures, as shown in Figure 9 for a sample collected at a stoichiometric ratio of 2.0. For all the

samples analyzed, there was weight loss recorded between 350–450 ℃, which was attributed to the release of water of crystallization due to the decomposition of unreacted $Ca[OH]_2$ in the collected sample [27]. Further weight loss was recorded between 550–750 ℃, which was attributed to the release of carbon during the decomposition of $CaCO_3$ in the sample [28]. The presence of $CaCO_3$, as also observed in FTIR analysis, was associated with the contamination during sample preparation. This forms part of the unreacted sorbent fraction in the final product. Over the range of temperatures used, the decomposition of the final desulfurization product follows the reaction path below:

- Between 350–450 ℃ (release of water of crystallization)

$$Ca[OH]_2 \rightarrow CaO + H_2O \uparrow \tag{12}$$

- Between 550–750 ℃ (release of carbon dioxide)

$$CaCO_3 \rightarrow CaO + CO_2 \uparrow \tag{13}$$

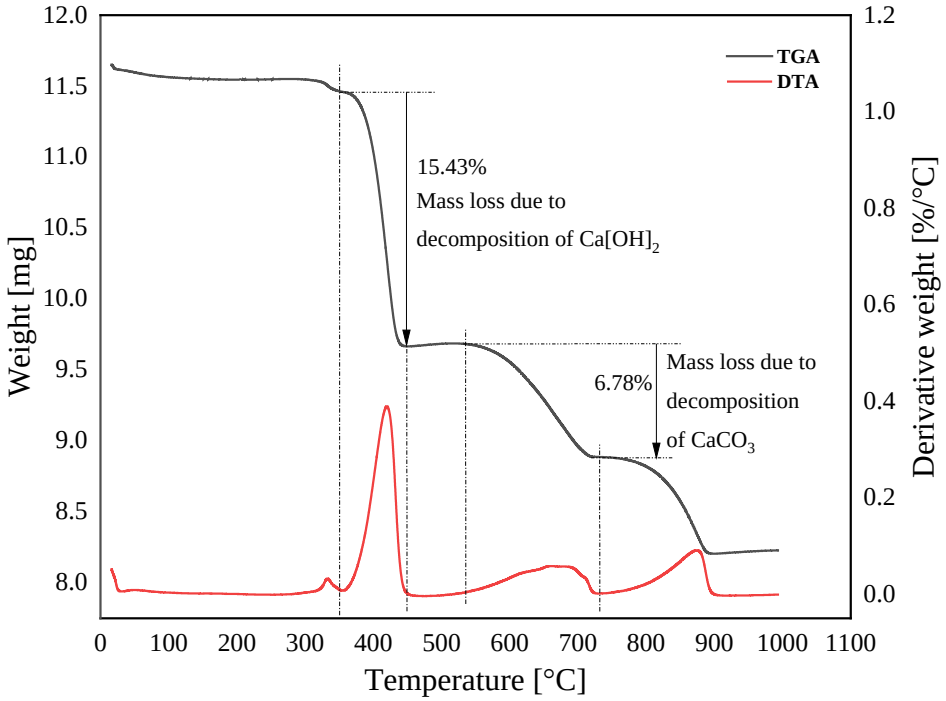

Figure 9. Thermogravimetry Differential Thermal Analysis (TG/DTA) curves for desulfurization product at a stoichiometric ratio of 2.0.

The content of unreacted $Ca[OH]_2$ in the final product was evaluated as [27]:

$$Ca[OH]_2\ content = \frac{MW of Ca[OH]_2}{MW\ of\ dehydrated\ water} \times wt.loss\ between\ 350 - 450℃ \tag{14}$$

$$Ca[OH]_2\ content = \frac{74}{18} \times 15.43 = 63.43\% \tag{15}$$

$CaCO_3$ content in the final product was evaluated as [28]

$$CaCO_3\ content = \frac{MW\ of\ CaCO_3}{MW\ of\ Carbon\ dioxide} \times wt.loss\ between\ 550 - 750℃ \quad (16)$$

$$CaCO_3\ content = \frac{100}{44} \times 6.78 = 15.41\% \quad (17)$$

Table 4. Final product composition under different stoichiometric ratios.

	$CaSO_3.\frac{1}{2}H_2O$	$Unreacted\ Ca[OH]_2$	SO_2 removal efficiency
SR=1.0	11.68%	46.87%	45%
SR=1.5	24.57%	41.23%	65%
SR=2.0	21.74%	63.43%	82%

Table 4 shows the evaluated compositions of gypsum and unreacted $Ca[OH]_2$ in the samples analyzed by TGA and XRF analysis. The results demonstrate that the samples collected for the experiment with an SR of 2.0 had the highest SO_2 removal efficiency of 82%. However, the analysis by TGA shows that it had a considerable amount of unreacted $Ca[OH]_2$ remaining in the final product. This reveals poor sorbent conversion at a high stoichiometric ratio. Both experiments conducted with SRs of 1.0 and 1.5 exhibited better sorbent conversion due to a lower concentration of unreacted $Ca[OH]_2$, but with relatively lower SO_2 removal efficiencies of 45 and 65%, respectively, as compared to the experiment conducted with an SR of 2.0. The analysis also shows higher concentrations of $CaSO_3.\frac{1}{2}H_2O$ for experiments with SRs of 1.0 and 1.5 compared to an SR of 2.0. The operating conditions at an SR of 1.5 yielded the highest concentrations of 24.57% for $CaSO_3.\frac{1}{2}H_2O$, which indicates better sorbent conversion.

5. Conclusion

An experimental study on the absorption of SO_2 from flue gas by means of a laboratory-scale spray dryer was carried out under different operating conditions. Results indicated decreased absorption of SO_2 at high inlet gas phase temperatures due to rapid evaporation. SO_2 absorption efficiency of up to 80% was achieved at an inlet gas-phase temperature of 120 °C. The experimental results revealed that a high absorption rate occurs just as the droplet leaves the nozzles due to the constant rate period within the spray chamber when the droplet is still wet. Results also indicated significant improvement of SO_2 absorption beyond 80% at high stoichiometric ratios due to reduced liquid-phase mass transfer resistances. Analysis of the degree of conversion of calcium indicated relatively better sorbent utilization at low stoichiometric ratios, with maximum utilization obtained at a Ca:S ratio of 1.5. TGA results generally indicated poor sorbent conversion in the spray dryer. The concentration of unreacted $Ca[OH]_2$ ranging from 41–64% in the final desulfurization product was achieved for experiments conducted with stoichiometric ratios ranging from 1.0–2.0. It is recommended that future studies investigate the impact of typical industrial flue gas components, including NO_x, SO_2, CO_2, O_2 and moisture, on the performance of spray drying in removing SO_2. Additionally, further research should explore other suitable sorbents for the spray drying process in FGD. These efforts will help to enhance the effectiveness of the spray drying method and improve its practical application in industrial processes.

Conflict of interest

The authors declare that they have no known competing financial interests or personal relationships that could have appeared to influence the work reported in this paper.

References

1. Córdoba P (2015) Status of Flue Gas Desulphurisation (FGD) systems from coal-fired power plants: Overview of the physic-chemical control processes of wet limestone FGDs. *Fuel* 144: 274–286. https://doi.org/10.1016/j.fuel.2014.12.065
2. Yang HM, Kim SS (2000) Experimental study on the spray characteristics in the spray drying absorber. *Environ Sci Technol* 34: 4582–4586. https://doi.org/10.1021/es001104c
3. Wang R, Dai Y, Zhang S, et al. (2019) Performance Evaluation and Optimization Analysis of Zero Discharge Device for Desulfurization Wastewater Based on Spray Drying Technology, IOP Conf. Ser.: Mater. Sci. Eng. 592:012199. https://doi.org/10.1088/1757-899X/592/1/012199
4. Carpenter AM (2012) Low water FGD technologies. *CCC/210 London: IEA Clean Coal Centre*. ISBN 978-92-9029-530-3
5. Katolicky J, Jicha M (2013) Influence of the Lime Slurry Droplet Spectrum on the Efficiency of Semi-Dry Flue Gas Desulfurization. *Chem Eng Technol* 36: 156–166. https://doi.org/10.1002/ceat.201100690
6. Shanshan Z, Renlei W, Guorui T, et al. (2020) Application and performance evaluation of desulfurization wastewater spray drying technology, *E3S Web of Conferences*, EDP Sciences 143: 02029. https://doi.org/10.1051/e3sconf/202014302029
7. Scala F, D'Ascenzo M, Lancia A (2004) Modeling flue gas desulfurization by spray-dry absorption. *Sep Purif Technol* 34: 143–153. https://doi.org/10.1016/S1383-5866(03)00188-6
8. Neathery JK (1996) Model for flue-gas desulfurization in a circulating dry scrubber. *AIChE J* 42: 259–268. https://doi.org/10.1002/aic.690420123
9. Partridge GP, Davis WT, Counce RM, et al. (1990) A mechanistically based mathematical model of sulfur dioxide absorption into a calcium hydroxide slurry in a spray dryer. *Chem Eng Commun* 96: 97–112. https://doi.org/10.1080/00986449008911485
10. Erdöl-Aydin N, Nasün-Saygili G (2007) Modelling of trona based spray dry scrubbing of SO2. *Chem Eng J* 126: 45–50. https://doi.org/10.1016/j.cej.2006.05.020
11. Hill F, Zank J (2000) Flue gas desulphurization by spray dry absorption. *Chem Eng Process Process Intensification* 39: 45–52. https://doi.org/10.1016/S0255-2701(99)00077-X
12. Hadjar H, Hamdi B, Jaber M, et al. (2008) Elaboration and characterisation of new mesoporous materials from diatomite and charcoal. *Microporous Mesoporous Mater* 107: 219–226. https://doi.org/10.1016/j.micromeso.2007.01.053
13. Garea A, Fernandez I, Viguri J, et al. (1997) Fly-ash/calcium hydroxide mixtures for SO2 removal: structural properties and maximum yield. *Chem Eng J* 66: 171–179. https://doi.org/10.1016/S1385-8947(96)03178-6
14. Lee KT, Bhatia S, Mohamed AR (2005) Preparation and characterization of sorbents prepared from ash (waste material) for sulfur dioxide (SO2) removal. *J Mater Cycles and Waste Manag* 7: 16–23. https://doi.org/10.1007/s10163-004-0121-2
15. Newton GH, Kramlich J, Payne R (1990) Modeling the SO2-slurry droplet reaction. *AIChE J* 36: 1865–1872. https://doi.org/10.1002/aic.690361210
16. Sahar A, Kehat E (1991) Sulfur dioxide removal from hot flue gases by lime suspension spray in a tube reactor. *Ind Eng Chem Res* 30: 435–440. https://doi.org/10.1021/ie00051a001

17. Mei D, Shi J, Zhu Y, et al. (2020) Optimization the operation parameters of SDA desulfurization tower by flow coupling chemical reaction model. *Pol J Chem Technol* 22: 35-45. https://doi.org/10.2478/pjct-2020-0006
18. Wey M, Wu H, Tseng H, et al. (2003) Experimental testing of spray dryer for control of incineration emissions. *J Environ Sci Health Part A* 38: 975–989. https://doi.org/10.1081/ESE-120018605
19. Wang D, Bao A, Kunc W, Liss W (2012) Coal power plant flue gas waste heat and water recovery. *Appl Energy* 91: 341–348. https://doi.org/10.1016/j.apenergy.2011.10.003
20. Zhang C, Zou D, Huang X, Lu W (2022) Coal-Fired Boiler Flue Gas Desulfurization System Based on Slurry Waste Heat Recovery in Severe Cold Areas. *Membr* 12: 47. https://doi.org/10.3390/membranes12010047
21. Scala F, Lancia A, Nigro R, et al. (2005) Spray-dry desulfurization of flue gas from heavy oil combustion. *J Air Waste Manage Assoc* 55: 20–29. https://doi.org/10.1080/10473289.2005.10464604
22. Ollero P, Salvador L, Cañadas L (1997) An experimental study of flue gas desulfurization in a pilot spray dryer. *Environ Prog* 16: 20–28. https://doi.org/10.1002/ep.3300160116
23. Küspert R, Krammer G (2012) Flue gases: Gypsum dewatering in desulphurisation. *Filtr Sep* 49: 30–33. https://doi.org/10.1016/S0015-1882(12)70144-1
24. Guan B, Fu H, Yu J, et al. (2011) Direct transformation of calcium sulfite to α-calcium sulfate hemihydrate in a concentrated Ca–Mg–Mn chloride solution under atmospheric pressure. *Fuel* 90: 36–41. https://doi.org/10.1016/j.fuel.2010.08.020
25. Böke H, Akkurt S, Özdemir S, et al. (2004) Quantification of CaCO3–CaSO3· 0.5 H2O–CaSO4· 2H2O mixtures by FTIR analysis and its ANN model. *Mater Lett* 58: 723–726. https://doi.org/10.1016/j.matlet.2003.07.008
26. Laperche V, Bigham JM (2002) Quantitative, chemical, and mineralogical characterization of flue gas desulfurization by-products. *J Environ Qual* 31: 979–988. https://doi.org/10.2134/jeq2002.9790
27. Kim T, Olek J (2012) Effects of sample preparation and interpretation of thermogravimetric curves on calcium hydroxide in hydrated pastes and mortars. *Transp Res Rec* 2290: 10–18. https://doi.org/10.3141/2290-02
28. VGB PowerTech (2008) Analysis of FGD Gypsum - VGB-Instruction Sheets - VGB Technical Rules, 2nd ed. VGB PowerTech e.V. Accessed: Aug. 02, 2021. Available: https://www.vgb.org/shop/technicalrules/merkblatter/m701e-ebook.html

AIMS Press